Shape Representation and Registration using Vector Distance Functions

Hossam Abd EL Munim and Aly A. Farag
Computer Vision and Image Processing Laboratory (CVIP)
University of Louisville, Louisville, KY 40292
{hossam,farag}@cvip.uofl.edu

Abstract

This paper introduces a new method for shape registration by matching vector distance functions. The vector distance function representation is more flexible than the conventional signed distance map since it enables us to better control the shapes registration process by using more general transformations. Based on this model, a variational frame work is proposed for the global and local registration of shapes which does not need any point correspondences. The optimization criterion can handle efficiently the estimation of the global registration parameters. A closed form solution is provided to handle an incremental free form deformation model for covering the local deformations. This is an advantage over the gradient descent optimization which is biased towards the initialization and is more time consuming. Results of real shapes registration will be demonstrated to show the efficiency of the proposed approach with small and large global/local deformations.

1. Introduction

The shape registration aims to build a point correspondence between a given shape (**source**) boundary and a template (**target**) [1, 2]. It is a very important process in computer vision and medical imaging. The registration depends on the : 1) method how to represent shapes, 2) nature of the transformation to move the points from the source towards the target, and 3) dissimilarity measure. The latter can be defined according to either the shape boundary or its entire region.

The iterative closest point algorithm was proposed in [3]. The approach is based on finding the correspondence based on the minimum distance criterion. Different shape registration approaches based on this technique are provided in the literature (e.g. [4]).

Shape registration is handled in [5] by matching signed distance functions. The dissimilarity measure allowed only the use of homogeneous scales which limits the efficiency of the process. Practically inhomogeneous scaling is necessary since data is gathered from different sources or subjects. The more general the transformation is, the better the results are.

A variational approach to top-down image segmentation was proposed in [6]. A projective transformation is used with a single prior image is embedded into the image to be segmented without using any point correspondences. The prior shape contour is represented by a cone. Perspective distortion and scaling of the visible contour are allowed using unlevel sections.

Cremers et.al. investigated the dissimilarity measures for shapes represented by the signed distance function [7]. A symmetric pseudo distance, which is not biased to small areas, was constituted as a dissimilarity measure. A shape-based segmentation technique was proposed which is pose invariant. Tracking of 2D and 3D objects' examples were demonstrated in [8] as well.

Different shapes registration approaches were proposed in the literature for example [9, 10, 11]. These approaches suffer from various problems, including scale variations and dependence on initialization. Also local deformations are not addressed efficiently.

Vector distance functions (VDF's) are used in [12] to evolve smooth manifolds. This representation defines a vector that connects any point in space to the nearest point on the curve or surface. This representation can deal with shapes of different dimensions.

We proposed shape representation by vector components in a different manner in our shape-based segmentation framework [13]. The vector components represent the vector projections from any point in space to the nearest point on the shape boundary. We give a positive sign to the points inside the shape and negative to those outside the shape to mark these regions. We used a simple dissimilarity measure to handle the problem of inhomogeneous scaling. Also the vector map was designed to handle the segmentation problem with the adaptive region model.

In this paper, we use the VDF shape representation as a similarity measure in the shape registration process. More general transformations with different scaling (s_x, s_y, s_z),

1-4244-1180-7/07/$25.00 ©2007 IEEE

rotation $(\theta_x, \theta_y, \theta_z)$,and translation (t_x, t_y, t_z) parameters will be used within a coordinate system of $x,\ y,\ and\ z$. The use of such vector functions results in a more adequate energy function which is optimized to achieve the transformation parameters both in the global and local registration schemes.

A variational framework for the registration process of shapes is formulated. The gradient descent optimization criterion is used to handle the global registration similar to that in [2]. The local deformations are covered using the incremental free form deformations. We do not use the gradient descent to estimate the control points positions. A closed form solution is developed for this purpose based on approximating the vector distance representation using the Taylor series expansion, leading to a linear system of equations. Promising results for synthetic and real shapes will be demonstrated.

The rest of the paper is organized as follows. Section 2 presents the shape representation formalism using the VDF. Global registration and alignment technique will be presented in Sec. 3. Sections 4 and 5 are dedicated to the local registration and control points positions calculation. The paper ends with a discussion and future research aspects in Sec. 6.

2. Shape Representation and the Vector Distance Function [14]

Given a smooth curve/surface V that represents boundaries of a given shape, the following implicit vector function is defined $\Phi:\ R^3 \rightarrow\ R^3$ where

$$\Phi(\mathbf{X}) = \mathbf{X}_0 - \mathbf{X}, \forall\, \mathbf{X} \in \Omega, \tag{1}$$

where $\mathbf{X}_0$ is the point on V with the minimum Euclidean distance to $\mathbf{X}$. A $2D$ example is given in Fig.1 for illustration. The surface points always satisfy the relation $|\Phi| = 0$.

If a global transformation is applied to the given shape represented by the designed vector map, one can predict the map of the new shape. We define a shape β that is obtained by applying a transformation $\mathbf{A}$ to a given shape α. Let us assume that the transformation has a scale matrix $\mathbf{S}$, rotation matrix $\mathbf{R}$, and translation vector $\mathbf{T}$. The transformation can be written for any point $\mathbf{X}$ in the space as $\mathbf{A} = \mathbf{SRX} + \mathbf{T}$.

Consider $\mathbf{X}, \mathbf{X}_0 \in \Omega_\alpha$ where the second point is the one with the minimum Euclidean distance on the surface to $\mathbf{X}$. Applying the transformation to the given points results in the pair of points $\hat{\mathbf{X}}, \hat{\mathbf{X}}_0 \in \Omega_\beta$. It is straightforward to show that:

$$\Phi_\beta(\mathbf{A}) = \hat{\mathbf{X}}_0 - \hat{\mathbf{X}} = \mathbf{SR}(\mathbf{X}_0 - \mathbf{X}) \tag{2}$$

and then the following relation holds:

$$\Phi_\beta(\mathbf{A}) = \mathbf{SR}\Phi_\alpha(\mathbf{X}) \tag{3}$$

showing that the proposed representation can give a vector similarity measure that includes inhomogeneous scales and rotations. Also it is invariant to the translation parameters. However the effect of scales and rotations can be predicted. This kind of measure overcomes the problem of using the conventional signed distance maps that leads to the use of homogeneous scales only.

Another issue is that the conventional level set function is not differentiable at the center line. Using this function to represent an **open** shape without sign as proposed in [15] will add another problem. By that definition, the function will not be differentiable at the boundary of the object. Then the registration formulation by minimizing an energy function of level sets differences using the gradient descent, is meaningless. In our case, the VDF has the desired characteristics around the object boundaries [12]. **It is smooth and differentiable at the boundaries**.

3. Global Registration of Shapes

Finding point-wise correspondences (between the two given shapes α and β) is the objective of the registration problem. An energy function is built based on the vector dissimilarity measure.

The VDF shape representation, changes the problem from the shape boundary domain to the higher dimensional vector representation. A transformation $\mathbf{A}$ that gives pixel-wise vector correspondences between the two shapes representations Φ_α and Φ_β, is required to be estimated.

The problem now can be considered as a global optimization that includes all points in the image domain. Some of squared differences will be considered with an energy optimized by the gradient descent approach.

3.1. Energy Formulation

According to the properties of the implicit vector representation shown above, the following dissimilarity measure is used:

$$\mathbf{r} = \mathbf{SR}\Phi_\alpha(\mathbf{X}) - \Phi_\beta(\mathbf{A}) \tag{4}$$

and the optimization energy function is formulated by the sum of squared differences as follows:

$$E(\mathbf{S}, \mathbf{R}, \mathbf{T}) = \int_\Omega \mathbf{r}^T \mathbf{r}\, d\Omega \tag{5}$$

The complexity of the problem is reduced by considering only points around the zero level of the vector function since far away points mapping can be neglected. The matching space is limited to a small band around the surface that can be selected by introducing the following energy function:

$$E(\mathbf{S}, \mathbf{R}, \mathbf{T}) = \int_\Omega \delta_\epsilon(\Phi_\alpha, \Phi_\beta)\mathbf{r}^T \mathbf{r}\, d\Omega \tag{6}$$

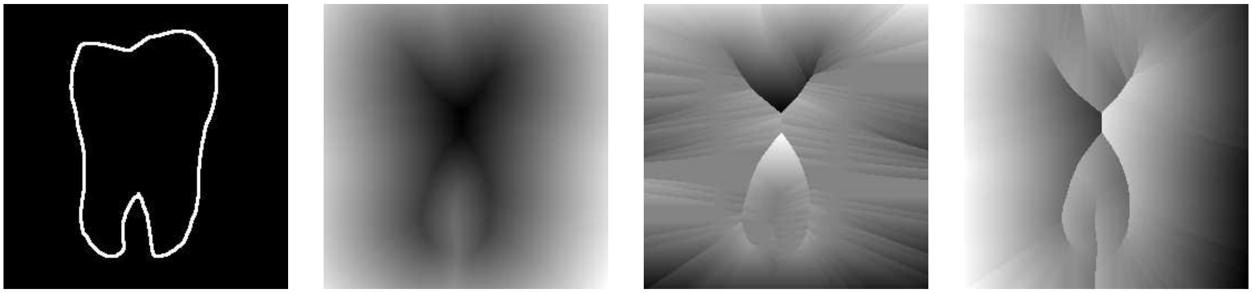

(a) (b) (c) (d)

Figure 1. Shape representation (gray level map):(a) A real tooth contour, (b) Conventional level set function, (c) The first projection of the proposed vector function (ϕ_1), (d) The second projection of the proposed vector function (ϕ_2).

where δ_ϵ is an indicator function defined as follows:

$$\delta_\epsilon(\Phi_\alpha, \Phi_\beta) = \begin{cases} 0 & \text{if} \quad min(|\Phi_\alpha|, |\Phi_\beta|) > \epsilon \\ 1 & \text{if} \quad min(|\Phi_\alpha|, |\Phi_\beta|) \leq \epsilon \end{cases} \tag{7}$$

The optimization of the given criterion is handled using the gradient descent method:

$$\begin{aligned} \frac{d}{dt}s &= 2\int_\Omega \delta_\epsilon \mathbf{r}^T[\nabla_s \mathbf{S}\mathbf{R}\Phi_\alpha(\mathbf{X}) - \nabla\Phi_\beta^T(\mathbf{A})\nabla_s\mathbf{A}]d\Omega \\ \frac{d}{dt}\theta &= 2\int_\Omega \delta_\epsilon \mathbf{r}^T[\mathbf{S}\nabla_\theta \mathbf{R}\Phi_\alpha(\mathbf{X}) - \nabla\Phi_\beta^T(\mathbf{A})\nabla_\theta\mathbf{A}]d\Omega \\ \frac{d}{dt}tr &= 2\int_\Omega \delta_\epsilon \mathbf{r}^T[\nabla\Phi_\beta^T(\mathbf{A})\nabla_{tr}\mathbf{A}]d\Omega \end{aligned} \tag{8}$$

where $s \in \mathbf{S}$, $\theta \in \mathbf{R}$, and $tr \in \mathbf{T}$.

3.2. Quantitative Validation

An experiment is carried out for 100 registration cases. Each case considers a source and a target shapes. The source is fixed and the target is generated by applying a transformation on the source. Parameters (S_x,S_y,θ,T_x,T_y) are created and selected randomly from the ranges $[0.8, 1.2]$, $[0.8, 1.2]$, $[-60^o, 60^o]$,$[-60, 60]$,$[-60, 60]$ respectively. These generated patterns are kept as a ground truth for each case. The gradient descent optimization is done to get a steady state estimate for each parameter associated with each registration case. The experiment was done for two sets of shapes (corpus callosum and hippocampus as shown in Fig 2). The algorithm shows successful results for the two hundred cases and the energy goes down smoothly with the increase of the iteration number until perfect alignment is achieved. The measurements show that the errors means and standard deviations (Table 1) are very appropriate and satisfactory small. The final registration emphasizes that for each experiment where the boundaries of the source and target shapes become very close to each other. The gradient descent successfully estimates the scales, rotations, and translations.

Another test is carried out on 29 MRI data sets by extracting their corpus callosum shapes from the mid sagittal section (see Fig. 3 left image). The image shows that the shapes initially have large global differences which is reduced dramatically after carrying out the registration (see the middle picture). We notice from the relation between S_x and S_y that they are almost different all the time. This justifies the use of the implicit vector representation for covering the inhomogeneous scales problem.

4. Local Registration of Shapes

The above registration works well for global registration of objects and can not handle local deformations. Following the work in [2], a local deformation vector $\mathbf{U} = [u_x\ u_y\ u_z]^T$ is applied to the globally transformed shape represented by $\hat{\alpha}$. The following dissimilarity measure is considered:

$$\mathbf{r}_n = \Phi_{\hat{\alpha}}(\mathbf{X}) - \Phi_\beta(\mathbf{X} + \mathbf{U}) \tag{9}$$

and hence the non rigid energy function will be defined as:

$$E_n(\mathbf{U}) = \int_\Omega \mathbf{r}_n^T \mathbf{r}_n d\Omega \tag{10}$$

The local deformations are smoothed by adding another term that includes their derivatives as follows:

$$E_n(\mathbf{U}) = \int_\Omega \mathbf{r}_n^T \mathbf{r}_n d\Omega + \lambda\int_\Omega(\nabla^2 u_x + \nabla^2 u_y + \nabla^2 u_z)d\Omega \tag{11}$$

As an interpretation, the energy contains a term for covering the local deformations and another for penalizing large derivatives. To make the addition homogeneous, we weight the second term by $\lambda \in R^+$.

The gradient descent of the parameters based on the above formulation is accomblished as follows:

$$\frac{d}{dt}u = -2\lambda\triangle u + 2\int_\Omega \mathbf{r}_n^T \nabla\Phi_\beta(\mathbf{A})^T\nabla_u \mathbf{U} d\Omega \tag{12}$$

where $u \in \{u_x, u_y, u_z\}$.

Unfortunately, the use of this form of local deformations does not guarantee proper handling of the registered shape because it can not preserve topology. Also, it results in scattered front points leading to an open surface which is not

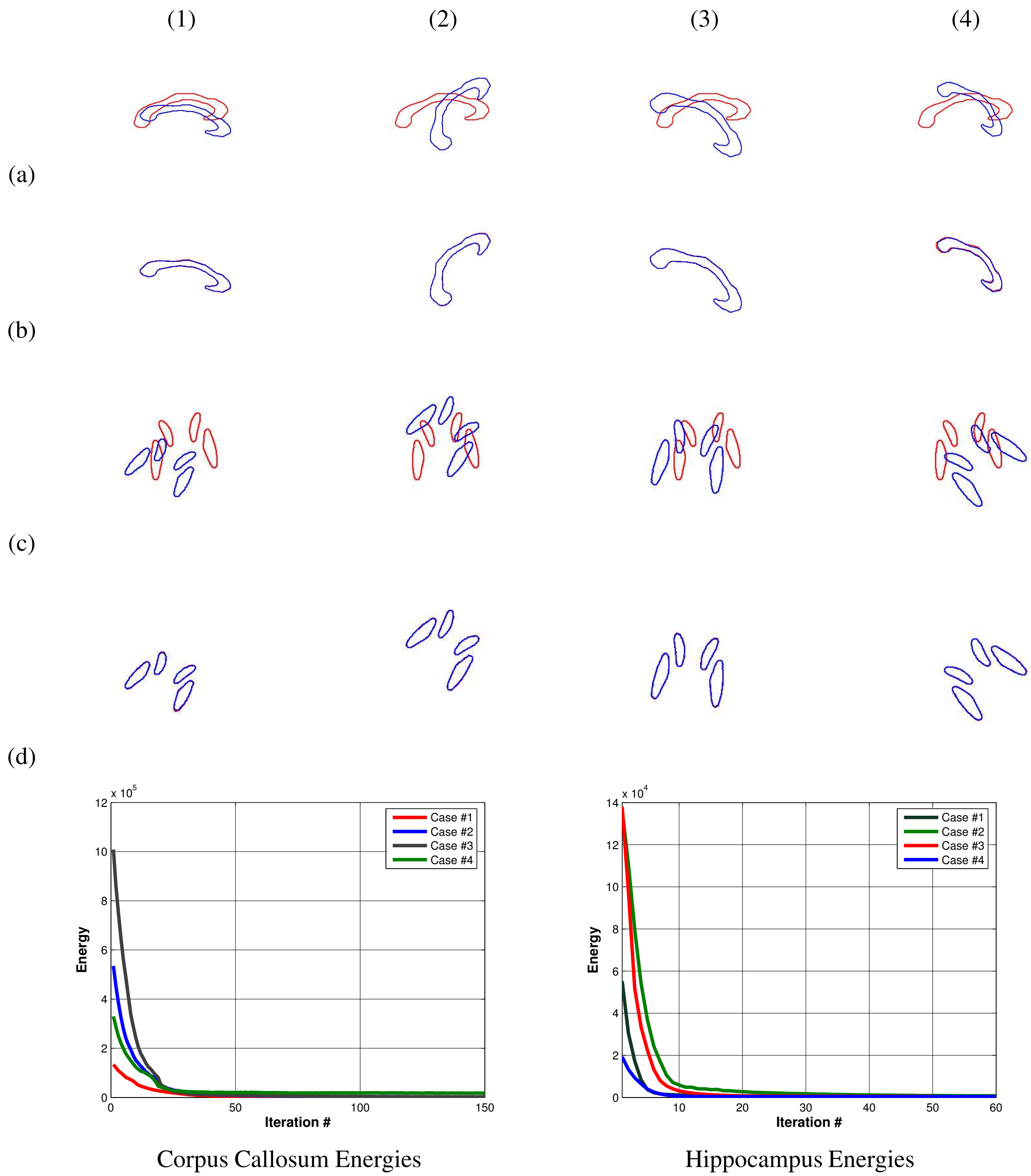

Figure 2. Corpus callosum and hippocampus shapes registration: (a) and (c) represent the initial position while (b) and (d) illustrate the final results. At the bottom, the energy function is plotted versus the iteration number for each case of the two shapes.

Table 1. Mean(μ) error and its standard deviation(δ) for the transformation parameters of the corpus callosum (CC) and hippocampus (HC) cases ($\mu \pm \delta$).

	S_x	S_y	θ^o	T_x	T_y
CC	-0.005 ± 0.009	0.003 ± 0.007	0.02 ± 0.18	-0.5 ± 0.4	-0.3 ± 0.5
HC	0.009 ± 0.007	0.005 ± 0.004	0.01 ± 0.09	0.0 ± 0.2	-0.0 ± 0.2

the case. Another issue is that the gradient descent does not guarantee the desired solution especially when using a large number of deformation vectors. The next section will solve this problem.

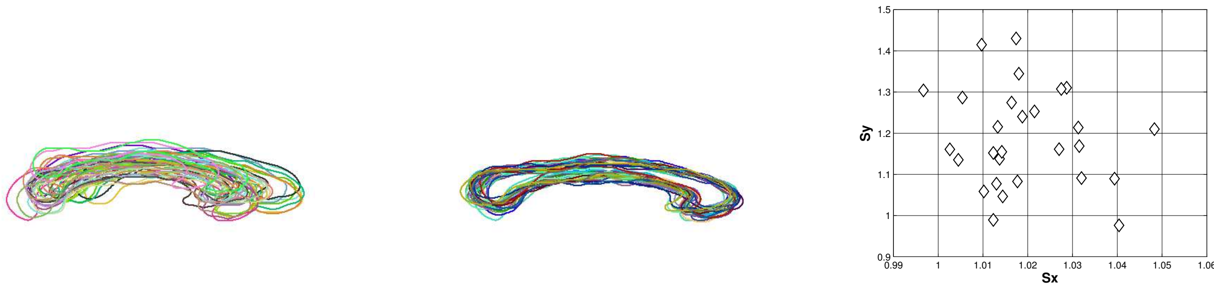

Figure 3. Different corpus callosum shapes registration (29 real shapes): Illustration before alignment is given in the left image while alignment results are shown in the middle. The relation between the horizontal and vertical estimated scales is plotted to the right.

5. Incremental Free Form Deformation (IFFD)

We use the incremental free form deformations to represent the local deformations [15]. The gradient descent is used to estimate the control points deformed positions based on the above formulation (to make it clear, we will formulate the $2D$ problem):

$$\frac{d}{dt}p = 2\int_{\Omega} \mathbf{r}_n^T (\nabla \Phi_\beta)^T \frac{\partial \mathbf{U}}{\partial p} d\Omega - 2\lambda \int_{\Omega} ((\frac{\partial^2 \mathbf{U}}{\partial x^2})^T \frac{\partial}{\partial p}(\frac{\partial^2 \mathbf{U}}{\partial x^2}) + (\frac{\partial^2 \mathbf{U}}{\partial y^2})^T \frac{\partial}{\partial p}(\frac{\partial^2 \mathbf{U}}{\partial y^2})) d\Omega \tag{13}$$

where $p \in \mathbf{P}_c$ which represents the lattice control points deformations vectors defined as follows:

$$\mathbf{P}_c = [P^x_{1,1}, \ldots, P^x_{n_x,n_y}, P^y_{1,1}, \ldots, P^y_{n_x,n_y}]^T \tag{14}$$

The control lattice size is $n_x \times n_y$ and the cubic splines representation of the deformation vector is defined by:

$$\mathbf{U} = \mathbf{U}(\mathbf{X}) = \sum_{l=0}^{3} \sum_{m=0}^{3} B_l(u) B_m(v) \mathbf{P}_{i+l,j+m} \tag{15}$$

Typical definition of i, j, u, v, B_l, B_m is found in [15]. For each level of the control lattice resolution, we assume that the amount of pixel deformation is relatively small such that its vector representation can be approximated using Taylor series expansion as follows:

$$\Phi_\beta(\mathbf{X} + \mathbf{U}) \approx \Phi_\beta(\mathbf{X}) + (\nabla \Phi_\beta(\mathbf{X}))^T \mathbf{U} \tag{16}$$

The control points are required to move and minimize the above objective function and hence satisfy the following condition:

$$\frac{\partial}{\partial p} E_n = 0 \tag{17}$$

By setting $\Phi(\mathbf{X}) = \Phi_{\hat{\alpha}}(\mathbf{X}) - \Phi_\beta(\mathbf{X})$, the above formulation will lead to:

$$\int_{\Omega} \Phi^T (\nabla \Phi_\beta)^T \frac{\partial \mathbf{U}}{\partial p} d\Omega = \int_{\Omega} ((\nabla \Phi_\beta)^T \mathbf{U})^T (\nabla \Phi_\beta)^T \frac{\partial \mathbf{U}}{\partial p} d\Omega - \lambda \int_{\Omega} ((\frac{\partial^2 \mathbf{U}}{\partial x^2})^T \frac{\partial}{\partial p}(\frac{\partial^2 \mathbf{U}}{\partial x^2}) + (\frac{\partial^2 \mathbf{U}}{\partial y^2})^T \frac{\partial}{\partial p}(\frac{\partial^2 \mathbf{U}}{\partial y^2})) d\Omega \tag{18}$$

The above equation is linear in terms of control points deformations. We can formulate the following linear system to give a closed form solution for the unknown deformations:

$$\mathbf{Q}\mathbf{P}_c = \mathbf{K} \tag{19}$$

The elements of the above matrix equation are estimated over the domain ($p = p_{row}$):

$$Q_{row,col} = \int_{\Omega} ((\nabla \Phi_\beta)^T \mathbf{U}')^T (\nabla \Phi_\beta)^T \frac{\partial \mathbf{U}}{\partial p} d\Omega - \lambda \int_{\Omega} ((\frac{\partial^2 \mathbf{U}'}{\partial x^2})^T \frac{\partial}{\partial p}(\frac{\partial^2 \mathbf{U}}{\partial x^2}) + (\frac{\partial^2 \mathbf{U}'}{\partial y^2})^T \frac{\partial}{\partial p}(\frac{\partial^2 \mathbf{U}}{\partial y^2})) d\Omega \tag{20}$$

$$K_{row} = \int_{\Omega} \Phi^T (\nabla \Phi_\beta)^T \frac{\partial \mathbf{U}}{\partial p} d\Omega \tag{21}$$

where $\mathbf{U}'$ is the cubic spline coefficient associated with the control point of the typical row and column of the equation.

Different elastic shape registration experiments are demonstrated in Fig. 4. In all the experiments, an initial lattice resolution of 7×7 is used, then the level is increased until a satisfactory deformation is achieved. Large local deformations are covered for the low resolution levels while fine details need higher resolution and so on. Another deformation example of open contour (teeth crowns or tags) is shown in Fig. 5. Investigating the point correspondence in each case, we find that: our algorithm gives exact physical dense correspondences, and the grid deformations do not have over-folding or crossovers which shows the necessity of the coarse to fine strategy and the added smoothing term weighted by λ. The step by step deformation is very important since it justifies that the change of the implicit representation due to the small movement can be approximated by the first order Taylor series expansion.

Compared to the approach proposed in [15], ours is more complicated but the proposed closed form solution for the control points positions is a great advantage. Unless we use the closed form solution, the total execution time will be doubled. Assume that the registration problem needs N incremental levels of free form deformations,

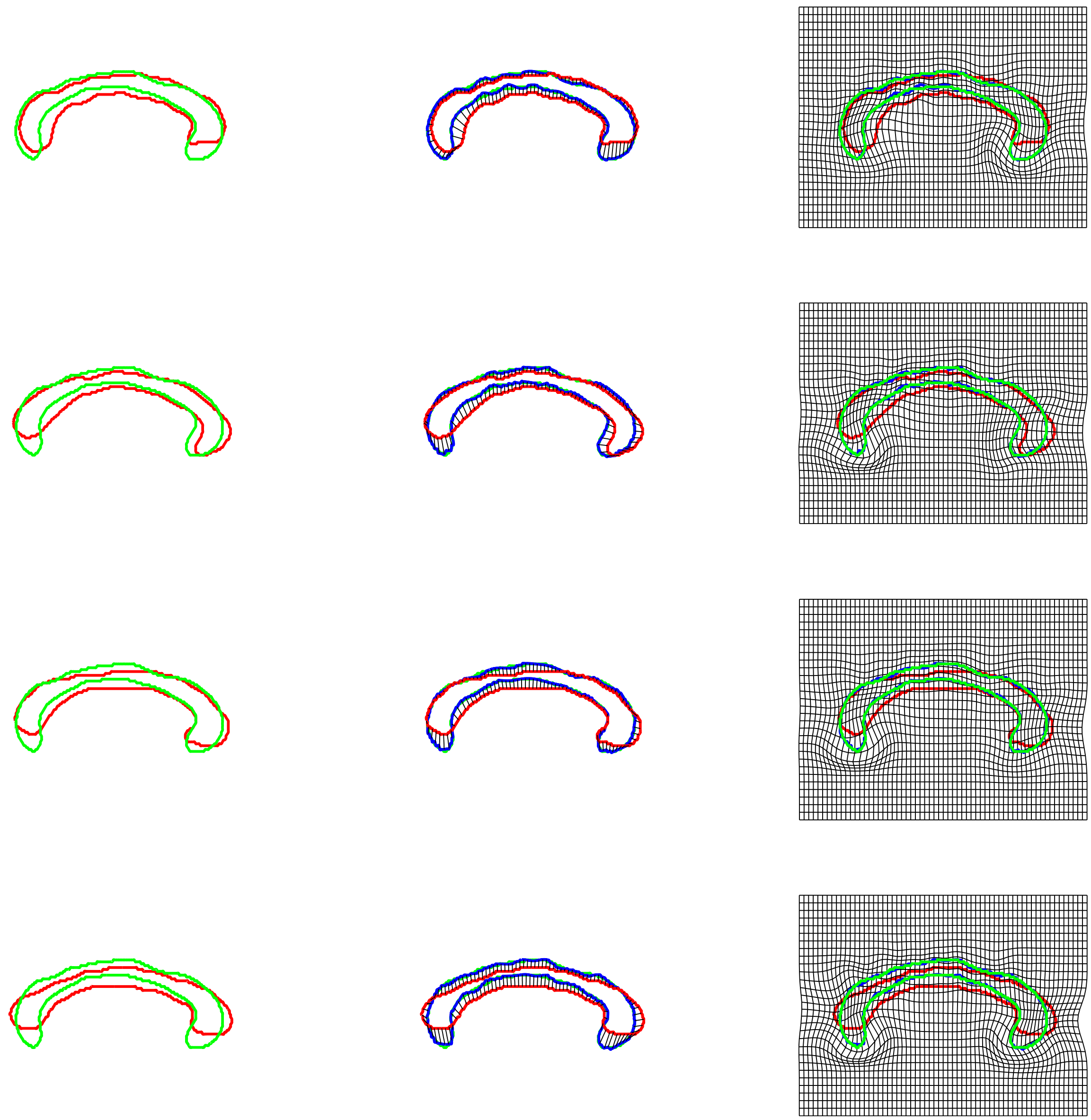

(a) (b) (c)

Figure 4. Different elastic registration examples of corpus callosum shapes (source contour is given in red, target contour is drawn in green, and deformed contour is shown in blue): (a) Initial position, (b) Final correspondences, and (c) Final grid deformation.

each level has $N_{CP} = n_x \times n_y$ control points, and hence $2 \times N_{CP}$ unknown variables ($x\ and\ y\ components$) for the gradient descent. If the average number of iterations of the gradient descent needed for each variable to reach the steady state is N_{Iter} with average time per iteration of Δt (with the method in [15]), the total time will be $Time_1 = \sum_{i=1}^{N}(2 \times N_{CP}^i * N_{Iter} \times \Delta t)$. For the same IFFD setup with the gradient descent of Eq. 13 which does not use the closed form solution, the total time will be doubled $Time_2 = \sum_{i=1}^{N}(2 \times N_{CP}^i \times N_{Iter} \times (2 \times \Delta t))$ because we use an implicit vector representation which has two components. The gradient descent execution time for an iteration will be roughly twice that of Δt. In case of applying the proposed closed form solution, the gradient descent iterations will be omitted. The new execution time can be estimated as $OurTime = \sum_{i=1}^{N}(2 \times N_{CP}^i \times (2 \times \Delta t))$. The time to construct the linear system of the closed form (Eq. 19) is equal to the time of one gradient descent iteration for all the variables. Our time holds the relation $OurTime = 2 * Time_1/N_{Iter}$. A good steady state solution for the gradient descent needs a number of iterations greater than 2 which guarantees that our execution time is less than that of the approach in [15].

6. Conclusion and Future Research

An efficient approach has been proposed for the shape registration problem. The technique depends on representing the shape implicitly in a higher dimensional vector function. It controls the registration process by using different scales in different coordinates directions. The VDF is used within an energy formulation that measures the dissimilarity between the source and target shapes representations. A variational scheme is proposed to calculate the registration parameters for both the global and local cases. Compared to the other conventional approaches:(1) Our results are promising and does not need any point correspondences, (2) Our approach can work for large and different scales without any problems, (3) The local deformations are handled by a closed form solution for the positions of the control points for each level of the IFFD. Regarding future work, applications like shape-driven segmentation and tracking will be involved to use the vector distance function.

7. Acknowledgement

This research has been supported by the National Science Foundation (NSF) Grant IIS-0513974.

References

[1] R. Veltkamp and M. Hagedoorn, “State of the Art in Shape Matching,“*Technical Report*, UU-CS-19999-27, Utrecht University, Sept. 19999.

[2] Nikos Paragios, Mikael Rousson and Visvanathan Ramesh, “Matching Distance Functions: A Shape-to-Area Variational Approach for Global-to-Local Registration,“*European Conference in Computer Vision*, Copenhagen, Denmark, Jun. 2002.

[3] P. Besl and N. Mckay, “A Method for Registration of 3-D Shapes,“*IEEE Tr. on PAMI*, 14(2):239–256, 1992.

[4] Z. Zhang, "Iterative Point Matching for Registration of Freeform Curves and Surfaces," *Ph.D. International Journal of Computer Vision*, vol. 13, no. 2, pp. 119152, 1994.

[5] M. Rousson, N. Paragios and R. Deriche. "Implicit Active Shape Models for 3D Segmentation in MRI Imaging," *Medical Image Computing and Computer Assisted Intervention (MICCAI)*, Part 1, pp 209–216, Saint-Malo, France, September 26-29, 2004.

[6] T. Riklin-Raviv1, N. Kiryati, and N. Sochen., “Unlevel-sets: geometry and prior-based segmentation,“*ECCV*, pages 50-61, 2004.

[7] D. Cremers and S. Soatto., “A Pseudo-distance for Shape Priors in Level Set Segmentation,“*2nd IEEE Workshop on Variational, Geometric and Level Set Methods in Computer Vision*, pages 169-176, 2003.

[8] D. Cremers, T. Kohlberger, C. Schnorr, “Shape statistics in kernel space for variational image segmentation,“*Pattern Recognition*, 36(9): 1929-1943, 2003.

[9] I. Cohen and I. Herlin, “Curve Matching Using Geodesic Paths,“*In IEEE CVPR*, pp 741–746,Santa Barbara, USA, 1998.

[10] A. Fitzgibbon, “Robust Registration of 2D and 3D Points Sets,“*In Proceeding of The British Machine Vision Conference (BMVC)*, vol. 2, pp 411–420,University of Manchester, UK, 2001.

[11] D. Kozinska, O. Tretika, J. Nissanov, and C. Ozturk, “Multidimensional Alignment Using the Euclidean Distance Transform,“*Graphical Models and Image Processing*, pp 6:373–385,1997.

[12] Jos Gomes and Olivier Faugeras, “The Vector Distance Functions,“*International Journal of Computer Vision*, 52(2-3): 161-187 (2003).

[13] H. E. Abd El Munim and A. A. Farag, “Curve/Surface Representation and Evolution using Vector Level Sets with Application to the Shape-based Segmentation Problem ,“ *Tenth IEEE Transaction on Pattern Analysis and Machine Intelligence (PAMI)*, Vol. 29, No. 6, pp. 945–958, June 2007.

[14] H. E. Abd El Munim and A.A. Farag, "A New Variational Approach for 3D Shape Registration," *Proceedings of International Symposium on Biomedical Imaging,* Metro Washington, D.C., USA, pp. 1324–1327, April 2007.

[15] Xiaolei Huang; Paragios, N.; Metaxas, D.N., “Shape registration in implicit spaces using information theory and free form deformations ,“*TPAMI*, Vol. 28, Issue 8, Aug. 2006 Page(s):1303-1318.

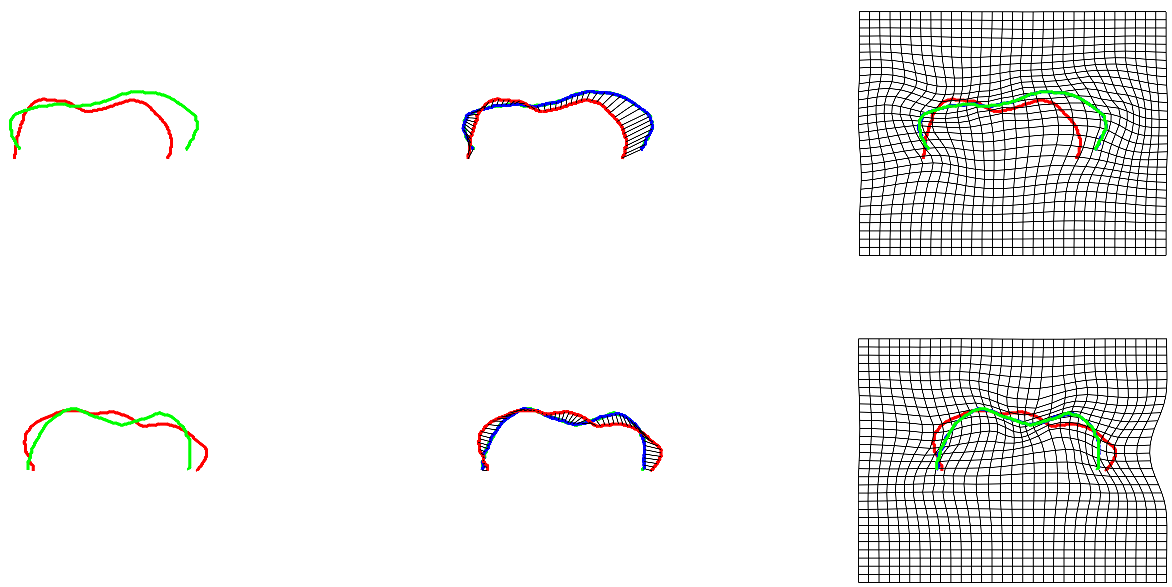

(a) (b) (c)

Figure 5. Different elastic registration examples of open shapes (source contour is given in red, target contour is drawn in green, and deformed contour is shown in blue): (a) Initial position, (b) Final correspondences, and (c) Final grid deformation.